International Journal of Engineering Research
Volume No.5, Issue No.11, pp : 847-850

ISSN:2319-6890)(online),2347-5013(print)
1 Nov. 2016

Liquefaction Potential Area Identification in Southern Bali Island Based on Ground Penetrating Radar, Geoelectricity and Borehole Data

Rahmat Nawi Siregar[1, a)] and Sismanto [1, b)]

[1]Department of Physics, Gadjah Mada University, Yogyakarta, Indonesia.

[a)]Corresponding author: rahmat.nawi.s@mail.ugm.ac.id, [b)]sismanto@ugm.ac.id

Abstract. The potential area of liquefaction in southern Bali Island has been identified by using ground penetrating radar, resistivity geoelectricity with dipole-dipole configuration, and borehole data. The research has been conducted in 16 GPR's sites, 12 geoelectricity lines, and 8 borehole points. The interpretations of GPR and geolectricity revealed the presence of sand-silt-clay with (5.00 – 23.6) Ω m resistivities at (0 – 5) meter depth and groundwater table with (0.265–17.1) Ω m at (0–7) meter depth. The measurement of sand diameter in Sanur, Sarangan, Tanjung Benoa and Tuban reveal that sand-silt-clay fraction which has < 20 % fines are categorized as highly potential liquefaction.

Keywords: Liquefaction, Ground Penetrating Radar, Geoelectricity, Borehole.

I. Introduction

Liquefaction is a phenomenon whereby a granular material transforms from a solid state to a liquefied state as a consequence of increase in pore water pressure [i]. This phenomenon induces post earthquake effect and stimulates damages to buildings for the next earthquake. There are some factors which contribute to liquefaction such as shallow groundwater (< 5 m) [ii], clean sand layer [iii], less than 20 % fines percentage [iv], 0.1 g ground acceleration and more than 5 SR earthquake magnitude [v]. Those factors produce more saturated soil when earthquake occurs.

Bali Island has high seismicity level in Indonesia and classified as vulnerable of earthquake. Seismic activity in southern Bali is controlled by subduction of Australia plate and Eurasia plate. Meanwhile, shallow seismicity activity on land is controlled by local faults in north and northeast of Bali Island. Generally, the directions of faults in Bali are northwest-southeast and west-east [vi].

The geological structure of southern Denpasar is controlled by alluvium sediment which consist of boulder, gravel, sand, silt and clay as a result of river, lake, and coastal material sedimentation. Regional geology is characterized as repetition of sand fraction from fines to gravel size with silt and clay within it. The depth of this quarter sediment is less than 20 meters [vii]. So, based on soil layers, southern Bali has a vulnerability to geological disaster, especially liquefaction.

Liquefaction potential index has been analyzed with geo-engineering methods such as Cone Penetrating Test and Standard Penetrating Test. However. In order to map a high quality subsurface condition, geophysical methods, Ground Penetrating Radar and Geoelectricity, had been applied. Physical properties – the ability to reflect or refract radar wave and the ability to induced by electricity – of sand, clay silt and water, will give the information for liquefaction possibilities. Ground penetrating radar (Georadar) is an active geophysical method by using radar wave range (1–1000 MHz) to describe shallow subsurface with high accuracy [viii]. Radar pulse which is transmitted by transmitter antenna is reflected and refracted by subsurface layer to receiver antenna. The geoelectricity method uses potential difference from electric current which is injected to the earth [ix]. This potential difference provides subsurface information about type and characteristics of electricity from each non-homogeneous layer.

II. Research Method

Georadar, geoelectricity with dipole–dipole's configuration, and borehole were applied in 36 sites around Denpasar City, Badung District from Mengwi Subdistrict to South Kuta.

Georadar measurments have been conducted by using GSSI (Geophysical Survey System Inc) SIR – 20 with transducer 200 MHz. The output was linescan wiggle and processed with GSSI RADAN software 5. Furthermore, radagrams profile are proceseed by Reflexwave software. Georadar data processing are started by changing radagram display from gray 1 to rainbow 2, then show the amplitude's bar. In order to put arrival time of first wave, static correction was applied. Henceforth, data are filtered by subtracts mean (dewow) 1 D filtering. This step is pointed out to reduce low frequency which is caused by any electronic device nearby measurement.

The next step is gain processing (depth function) in order to clarify the reflector shown in radagram. As a reflector was gained, so did the noises in radagram. The next step is band pass frequency filtering to reduce noises after gain processing. Frequency range of noises are sorted and eliminated, while signal frequency is kept. The next filtering is background removal 2 D or known as background subtraction. Noises which appear in profile are then reduced. Next, traces stack are applied

ISSN:2319-6890)(online),2347-5013(print)
1 Nov. 2016

to increase signal to noise ratio (S/N). This tracing step will brighten signal and decreasing signal's amplitude. The last processing step is F-K filter. This process filter temporal and spatial frequency, then gives outcome in frequency-wave number (k) function. Generally, F-K filter is used to eliminate coherent noise (noise from trace to trace along profile). GPR interpretation is based on Figure 1.

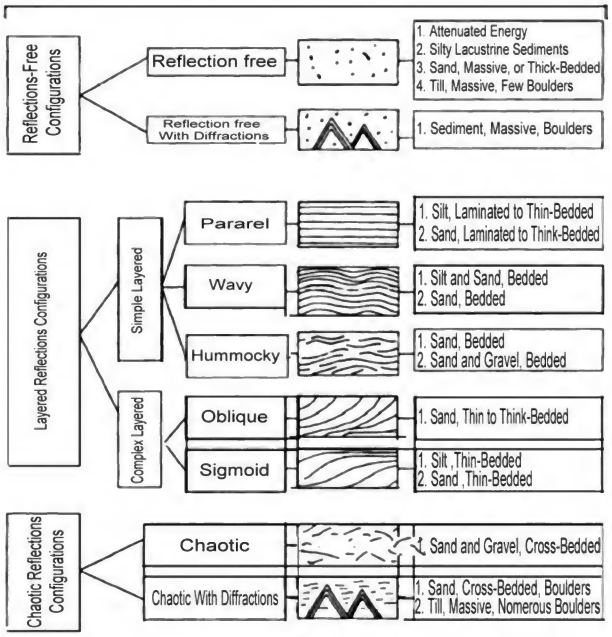

Figure 1. Subsurface interpretation based on radagram profile [x]

Geoelectricity measurement has been conducted by using multichannel Super String R8/IP with resistivity output in *stg digital format. Processing step is started by converting data from *stg as a raw data from resistivity multichannel Super String R8/IP instrumentation, to *dat format by using AGGIS Admin. Henceforth, the data are combined with topography data which are acquired by GPS Garmin. These data will become input data for each research sites in *dat notepad extention. Then, the input data are processed in to Earthimager 2DINV software, so resistivity's profile of measurement and calculation are obtained.

III. Results

Sarangan area

Radagram profile of Sarangan's site is ahown in Figure 2. Upper layer at (0-3) meter depth shows different reflectors configuration from (100-200) meter which is dominated by parallel simple layered configuration indicating the presence of sand bedded. From (141-179) meter and (0-1.5) meter depth, parallel layer has high amplitude continuity with radar propagation velocity of (4.36-5.95) cm/ns, predicted as highly saturated sand.

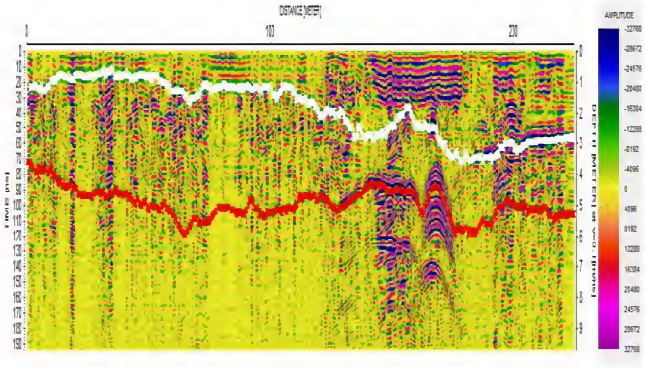

Figure 2. Radagram profile of Sarangan's site

Second layer from (3-5) meter depth shows wavy simple layer reflection from (100-200) meter which indicating sand and silt pattern. From (162-168) meter and (3.7-6.02) meter depth, clearly shows hyperbola reflector with radar wave velocity of 12.68 cm/ns and predicted as pipe. It is used to flow water, shown with high amplitude and hyperbola form with the velocity is (2.73-3.64) cm/ns. From (184-250) meter and (3-5) meter depth, indicating the presence of groundwater table with high amplitude continuity and the velocity is (3.12-3.64) cm/ns.

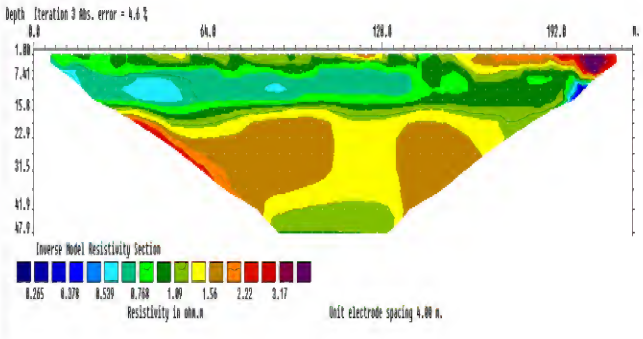

Figure 3. Resistivity profile of Sarangan site

Geoelectricity profile (Figure 3) shows low resistivity range (0.265-3.17) Ω m. From (0-140) meter and (7-15) meter depth shows greenish domination with (0.539-0.768) Ω m resistivity and interpreted as low permeability layer. The (0-3) meter depth shows green domination with 1.09 Ω m resistivity and interpreted as saturated sand. From (192-216) meter and (0-3) meter depth clearly shows the domination of of red-purple with (2.22-3.17) Ω m and predicted as groundwater.

Borehole data present the percentage of sand fines diameter (0.075-1) mm (liquefaction's condition) reaches 50% as shown in Figure 4. Based on radagram and resistivity profile along Sarangan's site at (3-4) depth indicate the presence of water saturated sand with diameter from (0.075-0.15) mm and 13% of percent fines. This phenomenon indicates that soil layer at (1.50-1.95) meter depth had potency for liquefaction.

doi : 10.17950/ijer/v5s11/1103

ISSN:2319-6890)(online),2347-5013(print)
1 Nov. 2016

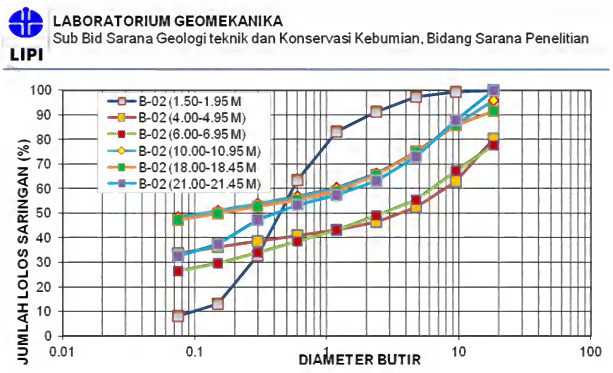

Figure 4. Sand size distribution of Sarangan site

Jimbaran area

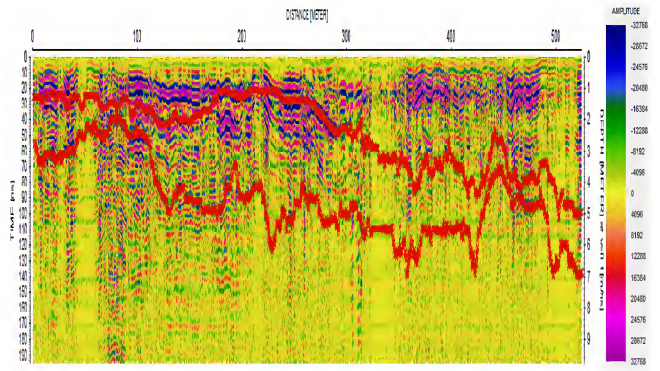

Figure 5. Radagram profile of Jimbaran site

Upper layer at (0-5) meter depth (Figure 5) shows reflectors configuration from (100-200) meter which is dominated by parallel simple layered configuration indicating the presence of sand-silt and groundwater. Radar wave velocities are (6.50-12) cm/ns. From (300-500) meter, reflection free configuration shows high energy attenuation which is caused by boulders, interpreted as limestone with radar propagation (7.43-17.33) cm/ns. Second layer from (5-7) meter depth shows chaotic reflection with diffraction indicating sand and limestone pattern. Radar wave propagation (13.50-15.39) cm/ns, defined as radar wave propagation on limestone and dry sand.

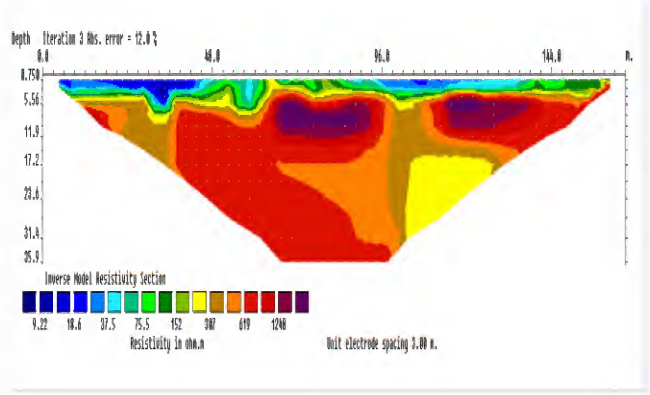

Figure 6. Resistivity profile of Jimbaran site

Geoelectricity profile (Figure 6) at (99-162) meter distance and (0-6) meter depth shows high resistivity range (75.7-151) Ω m. Based on radagram profile, layer with those resistivities are limestone. From (7-15) meter depth shows resistivity range (307-1248) Ω m and interpreted as limestone.

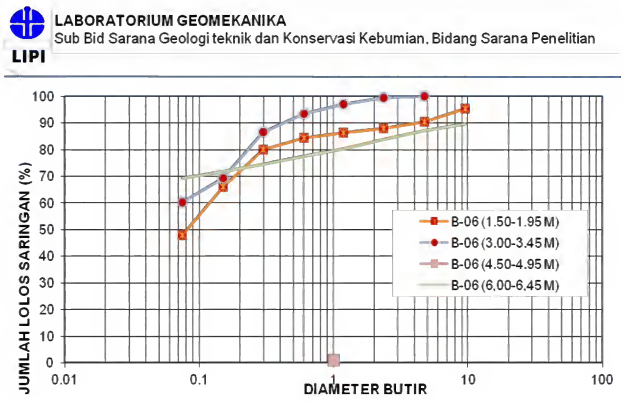

Figure 7. Sand size distribution of Jimbaran site

Distribution of Liquefaction Potential Area of Southern Bali Island

Based on size and characteristic of soil, the distribution of clay-silt have liquid limit 81.92%-158.15%, plasticity limite 42.5%-72.38%, plasticity index 29.72%-102.26% which are investigated into potential liquefaction. That's why, clay-silt fraction is classified into ML-MH (Figure 8) based on Unified Soil Classification System (USCS).

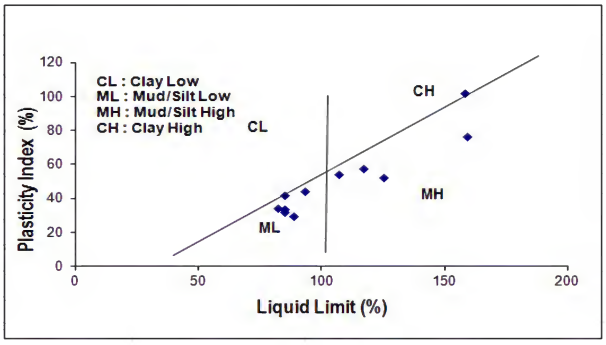

Figure 8. Relation between liquid limit and plasticity index from soil samples

Identification of liquefaction potential area based on georadar, geoelectricity and borehole data from southern Bali island indicate that Sanur, Sarangan, Tanjung Benoa and Tuban have high liquefaction possibility. It is caused by sand-silt

doi : 10.17950/ijer/v5s11/1103

ISSN:2319-6890)(online),2347-5013(print)
1 Nov. 2016

material haw >20% fines and categorized as very easily liquefy with groundwater (2-5) meter depth as shown in Figure 9.

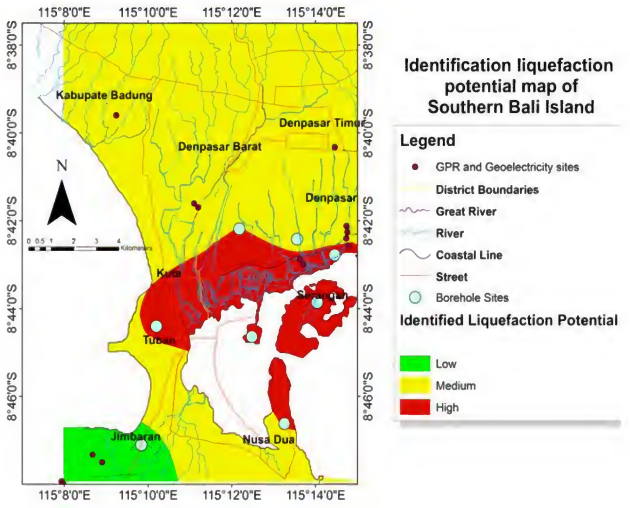

Figure 9. Distribution map of identified liquefaction potential area

IV. Conclusion

Subsurface structures of southern Bali island are consist of sand, clay and silt with resistivity range from (5-23.6) Ω m and the presence of groundwater with resisitivity of (0.265-17.1) Ω m. Subsurface structures of Jimbaran are dominated by limestone (50-200 Ω m) as a coastal alluvium lifting from geological south formation. Interpretation of radagram resistivity and borehole data identified Sanur, Sarangan, Tanjung Benoa and Tuban as high potential liquefaction area.

Acknowledgments

This work was supported by Ministry of Energy and Mineral Resource for Geological Survey Department, Bandung. The financial support from Indonesian Directorate General of Higher Education (DIKTI) through BPP-DN Scholarship No. 1414.59/E4/4/2013 are thankfully acknowledge. The author wish to thanks the directors of Publishing and Publication Department of Gadjah Mada University for permission to publish this article. Thankfully to Ir. Eko Soebowo from Indonesian Institute of Science for Geotechnology Research Center for his help and permission during data analysis. Thanks are due to all field staff for their cooperation and supports during field works and data analysis.

References

i. *J. Karthikeyan and P. Samui., Determination of Strain Energy for Triggering Liquefaction Based on Gaussian Process Regression, Engineering Journal* ***17****, 72-78 (2013)*

ii. *W. Pawirodikromo, "Likuifaksi (Liquefaction)" in Seismologi Teknik dan Rekayasa Kegempaan (Pustaka Pelajar, Yogyakarta, 2012), pp 558-565.*

iii. *I. Towhata, K. Gunji and Y.A. Hernandez," Laboratory tests on cyclic undrained behavior of loose sand with cohesionless silt and its application to assesment of seismic performance of subsoil" in Soil Liquefaction during Recent Large-Scale Earthquakes, edited by R.P. Orense (Taylor and Francis Group, London, 2014), pp 79 – 83.*

iv. *V.G. Perlea, J.P. Koester and Prakash, How Liquefable are cohesive soils?, Proceeding Second International Conference on Earthquake Geotechnical Engineering,* ***2****, 611-618 (1999)*

v. *K. Kumar, "Site Seismicity, Seismic Soil Response and Design Earthquake" in Basic Geotechnical Earthquake Engineering (New Age International Publishers, New Delhi, 2008), pp 52-56.*

vi. *R. McCaffrey and J. Nabelek, "Earthquakes, Gravity and the Origin of the Bali Basin : An Example of a Naschent Continental Fold and Thrustbelt", Journal of Geophysical Research,* ***92****, 441-460 (1987).*

vii. *E.Soebowo, D. Sarah, Y. Kumoro and N.A. Satriyo, Identifikasi Zona Penurunan Tanah Akibat Likuifaksi di Daerah Serangan-Tanjung Benoa Bali Selatan, Proceeding Pemaparan Hasil Penelitian Puslit Geoteknologi LIPI,* ***1****, 193-196 (2011).*

viii. *H.M. Jol, "Electromagnetic Principles of Ground Penetrating Radar" in Ground Penetrating Radar : Theory and Applications (Elsevier, Oxford, 2009), pp 5-8.*

ix. *P.Kearey, M.Brooks and I. Hill, "Electrical Surveying" in An Introduction to Geophysical Exploration Third Edition (Blackwell Publishing, London, 2002), 183-186.*

x. *M. Beres, and F.P., Haen, "Application of Ground Penetrating Radar Methods Hydrogeologic Studies, Ground Water", 1991, Vol. 3, 375-386.*